Photodiagnosis and Photodynamic Therapy 27 (2019) 354–361

Contents lists available at ScienceDirect

Photodiagnosis and Photodynamic Therapy

journal homepage: www.elsevier.com/locate/pdpdt

Ex-vivo analysis of quantitative 5-ALA fluorescence intensity in diffusely infiltrating gliomas using a handheld spectroscopic probe: Correlation with histopathology, proliferation and microvascular density

Mauricio Martínez-Moreno[a,1], Barbara Kiesel[a], Adelheid Woehrer[b], Mario Mischkulnig[a], Julia Furtner[c], Gerald Timelthaler[d], Walter Berger[d], Engelbert Knosp[a], Johannes A. Hainfellner[b], Stefan Wolfsberger[a], Georg Widhalm[a,d,*]

[a] Department of Neurosurgery, Medical University of Vienna Waehringer Guertel 18 – 20, 1090 Vienna, Austria
[b] Institute of Neurology, Medical University of Vienna Waehringer Guertel 18 – 20, 1090 Vienna, Austria
[c] Department of Biomedical Imaging and Image-guided Therapy, Medical University of Vienna Waehringer Guertel 18 – 20, 1090 Vienna, Austria
[d] Institute of Cancer Research, Medical University of Vienna Waehringer Guertel 18 – 20, 1090 Vienna, Austria

ARTICLE INFO

Keywords:
Brain glioma
5-ALA fluorescence
Handheld probe
Spectroscopy
Histopathology
Proliferation rate
Microvessel density

ABSTRACT

Background: Intraoperative semiquantitative classification of different visible 5-aminolevulinic acid (5-ALA) fluorescence levels by the neurosurgeon is subjective. Recently, handheld spectroscopic probes were introduced enabling quantitative analysis of 5-ALA induced fluorescence intensity (FI). The aim of this *ex-vivo* study was to correlate the FI in gliomas of different grades with histopathology, proliferation and microvasular density (MVD).

Patients and Methods: Patients with suspected World Health Organization (WHO) grade II-IV gliomas were included and tissue samples from different visible fluorescence levels (strong, vague or none) were intraoperatively collected. After resection, the FI of each sample was investigated *ex-vivo* by a handheld spectroscopic probe. The FI values were correlated with visible fluorescence, histopathology (WHO grade, quality of tissue, histopathological parameters of anaplasia), proliferation (MIB-1) and MVD.

Results: Altogether, 143 tumor samples with strong (n = 61), vague (n = 21) and no fluorescence (n = 61) were collected in 68 patients. We found significantly different median FI values between all three visible fluorescence levels. Moreover, the median FI value was significantly higher in WHO grade III/IV samples and compact tumor tissue compared to WHO grade II samples and infiltrated tumor tissue. Further, significant differences in median FI values were observed in specific histopathological parameters of anaplasia (mitotic rate, cell density, nuclear pleomorphism and microvascular proliferation) in multivariable analysis. Finally, a significant correlation between the proliferation rate and FI, but not between MVD and FI was noted.

Conclusion: Our data indicate that handheld spectroscopic probes are capable of visualizing intratumoral glioma heterogeneity by objective assessment of fluorescence and may thus optimize future glioma surgery.

1. Introduction

Diffusely infiltrating gliomas are the most common primary central nervous system tumors and are classified according to specific histopathological criteria in three glioma grades (WHO grades II-IV) [1–3]. These tumors are characterized by intratumoral heterogeneity with regard to histopathology, proliferation and microvasular density (MVD) [4–9]. In the last years, there exists mounting evidence that maximum safe resection of gliomas is associated with improved patient prognosis [6,10–13]. During glioma resection, precise tissue sampling is crucial to avoid potential histopathological undergrading and thus inadequate postoperative treatment [14,15].

* Corresponding author.
E-mail addresses: mauricio.martinezmoreno@helios-gesundheit.de (M. Martínez-Moreno), barbara.kiesel@meduniwien.ac.at (B. Kiesel), adelheid.woehrer@meduniwien.ac.at (A. Woehrer), mario.mischkulnig@meduniwien.ac.at (M. Mischkulnig), julia.furtner@meduniwien.ac.at (J. Furtner), gerald.timelthaler@meduniwien.ac.at (G. Timelthaler), walter.berger@meduniwien.ac.at (W. Berger), engelbert.knosp@meduniwien.ac.at (E. Knosp), johannes.hainfellner@meduniwien.ac.at (J.A. Hainfellner), georg.widhalm@meduniwien.ac.at (G. Widhalm).
[1] Permanent address: Clinic for Neurosurgery, Helios Clinics of Schwerin, Wismarscher Strasse 397, 19049, Schwerin, Germany.

https://doi.org/10.1016/j.pdpdt.2019.05.013
Received 9 January 2019; Received in revised form 2 May 2019; Accepted 13 May 2019
Available online 16 May 2019
1572-1000/

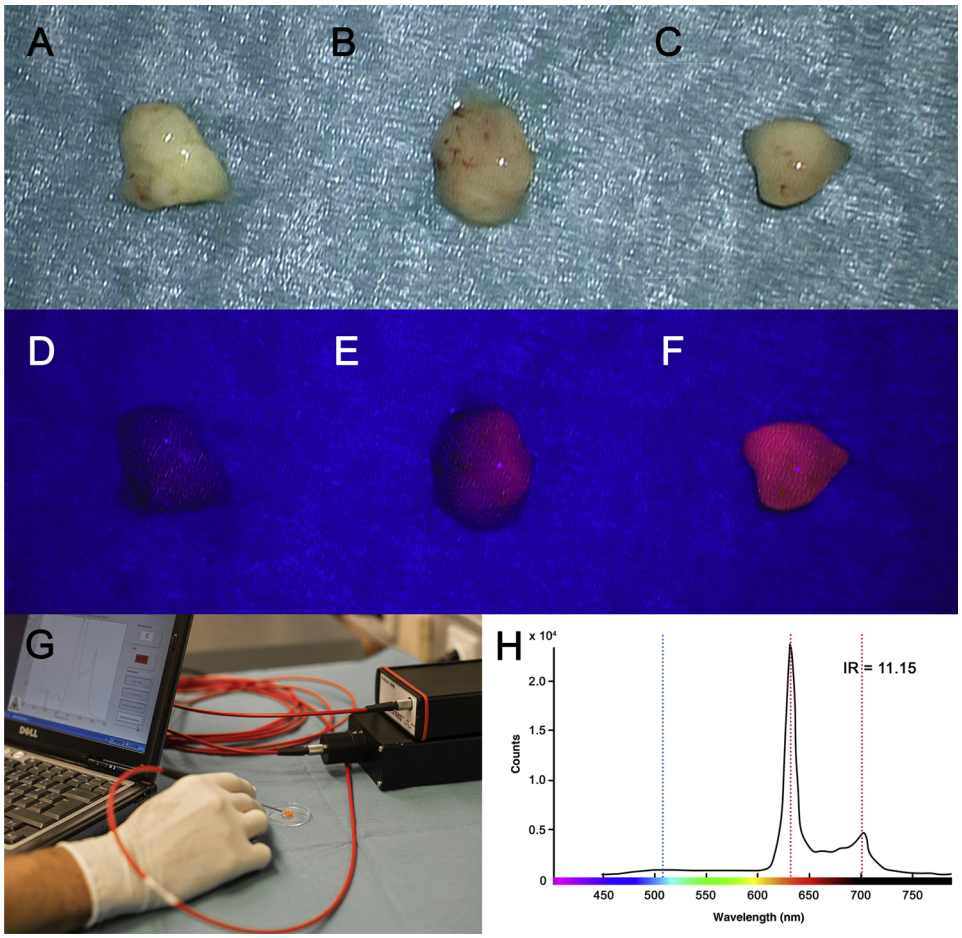

Fig. 1. Ex-vivo analysis of visible fluorescence and quantitative fluorescence intensity with a handheld spectroscopic probe in tumor samples from 5-ALA fluorescence-guided surgery.
(A, B, C) Three different tumor samples are investigated *ex-vivo* after surgery for visible fluorescence under white-light microscopy. Under violet-blue excitation light, (D) the first sample shows no fluorescence, (E) the second sample demonstrates vague fluorescence and (F) the third sample reveals strong fluorescence. Please note the characteristic two peaked emission spectrum of protoporphyrin IX. (G) With the assistance of a handheld spectroscopic probe, (H) the fluorescence intensity is measured in these samples. Please note the characteristic two-peaked emission spectrum of protoporphyrin IX.

Fluorescence-guided surgery using 5-aminolevulinic acid (5-ALA) is increasingly applied worldwide for improved visualization of brain tumor tissue and intratumoral heterogeneity in glioma surgery [16–20]. To this end, preoperative administration of 5-ALA results in accumulation of the fluorescent heme metabolite protoporphyrin IX (PpIX) in glioma tissue [21–23]. With the assistance of a modified neurosurgical microscope, three fluorescence levels (strong, vague or none) can usually be distinguished by the neurosurgeon during such procedures [24–26]. Recently, we were able to demonstrate that these three fluorescence levels correlate with distinct histopathological parameters, proliferation and MVD [27]. However, intraoperative assessment of these fluorescence levels by the neurosurgeon is observer dependent and thus subjective.

To allow objective assessment of PpIX fluorescence, handheld spectroscopic probes have been introduced to the neurosurgical field in the last years [28–34]. Such devices are capable to quantitatively measure PpIX fluorescence intensity (FI) in tumors, thereby providing an objective assessment of tissue fluorescence. Furthermore, such spectrometers have demonstrated to significantly improve detection of brain tumor tissue in comparison to conventional visual fluorescence [17,36,37]. However, a detailed correlation of quantitative PpIX fluorescence with histopathological parameters, proliferation and MVD in newly diagnosed diffusely infiltrating gliomas is still missing. These data would be crucial for reliable intraoperative application of such handheld spectrometric probes for precise tissue sampling in glioma surgery and thus optimized postoperative patient management.

The aim of our *ex-vivo* study was thus to clarify if such handheld spectroscopic probes are capable to objectively detect histopathological heterogeneity in gliomas. For this purpose, we collected tissue samples of different visible 5-ALA fluorescence levels in a large and homogenous cohort of patients with resection of a newly diagnosed diffusely infiltrating glioma (WHO grades II-IV). Subsequently, the FI of each tissue sample was quantitatively assessed by spectroscopic *ex-vivo* analysis. Finally, these FI values were correlated with (1) visible fluorescence, (2) histopathology (WHO grade, quality of tissue and histopathological parameters of anaplasia), (3) proliferation and (4) MVD.

2. Patients and methods

We prospectively collected data from patients with resection of a suspected newly diagnosed diffusely infiltrating glioma (WHO grades II-IV) with assistance of 5-ALA fluorescence and subsequent spectroscopic *ex-vivo* PpIX tissue analysis between January 2013 and 2015. This study was approved by the local ethics committee of the Medical University Vienna and patients provided a written consent.

2.1. Study cohort

According to a diagnostic magnetic resonance imaging (MRI) of the brain with administration of contrast-medium only patients with a suspected diffusely infiltrating glioma were included. The pattern of MRI contrast-enhancement of each tumor was classified as none, patchy/faint, focal, nodular and ring-like as described previously [38]. Patients with any previous treatments with resection or biopsy, chemotherapy and/or radiotherapy were excluded from this study.

2.2. ALA surgery and visible fluorescence

All patients of our study received a standard dose of 5-ALA (20 mg/kg bodyweight) approximately 3 h prior to surgery. To visualize

potential PpIX fluorescence, an adapted neurosurgical microscope was utilized (OPMI Pentero 900, and NC4, Carl Zeiss GmbH, Oberkochen, Germany). Glioma resection was assisted by neuronavigation and 5-ALA fluorescence. Dependent on the tumor localization, we used navigation with diffusion tensor imaging (DTI), intraoperative monitoring and/or awake surgery to limit the glioma resection. During surgery, multiple intratumoral tissue samples were safely collected by the neurosurgeon. Each tissue sample was semiquantitatively classified by the neurosurgeon as strong, vague or no fluorescence. For spectroscopic *ex-vivo* analysis, all collected samples were stored in light-protected vials with artificial cerebrospinal fluid. All patients were protected from light sources for a minimum time period of 24 h after 5-ALA administration to avoid potential skin phototoxicity.

2.3. Quantitative 5-ALA fluorescence intensity

Immediately after surgery, all collected tissue samples were analyzed *ex-vivo* by an adapted fiber-optic based spectrometry system (see Fig. 1) similar to that described by Haj-Hosseini et al. [31]. The spectroscopic system consisted of a laser source (ZM18H, Z-laser, Germany) with maximal excitation light at 405 nm, a sub-miniature A (SMA) fiber optic connector and a spectrometer with an optic filter (AvaSpec-2048 L, Avantes, The Netherland). A handheld fiber optic reflection probe with small tip (Avantes, The Netherlands) was used to direct the excitation light from six peripheral illuminating fibers to the specimen's surface. The reflected light was guided to the spectrometer by one fiber in the center of the probe. The spectrometer was connected to a computer with a dedicated software for calculation of FI, which was then instantly indicated as arbitrary units (a.u.) in a light spectrum curve. The excitation laser was pulsed electronically and synchronized with the integration time of the spectrometer, which minimizes photobleaching and maximizes the fluorescence signal. Additionally, the reflected fluorescence spectrum was integrated separately by the spectrometer during both on and off periods. Based on a pilot analysis prior to this study, an optimal output value of the laser source of 85% was determined and applied in the present study. During the spectroscopic analysis, the highest FI value was recorded for each tissue sample. The spectroscopic analysis required less than 10 s per tissue sample. After *ex vivo* analysis, all samples were placed in 10% formaldehyde and sent to the Institute of Neurology (Neuropathology) for routine histopathological work-up.

2.4. Tumor diagnosis

All collected tissue samples were embedded in paraffin and routinely processed for further histopathological analysis. The histopathological diagnosis of each tumor was routinely established by the local neuropathology team according to the applicable histopathological WHO criteria at time of diagnosis [39].

2.5. Histopathology

Additionally, the WHO grade, quality of tissue and histopathological parameters of anaplasia were assessed in each collected sample by two experienced neuropathologists (A.W., J.A.H.). The neuropathologists were blinded to clinical, radiological and fluorescence data.

2.5.1. WHO grade

First of all, the WHO tumor grade of each tissue sample was investigated according to the histopathological WHO criteria (WHO grades II, III or IV) [39].

2.5.2. Quality of tissue

The quality of tissue (tissue cytoarchitecture) of each sample was classified as compact tumor tissue or diffusely infiltrated tumor tissue as described previously [38]. Compact tumor tissue was defined as presence of densely packed cellular elements forming tumor nests. In contrast, diffusely infiltrated tissue was considered when less cell-dense tumor areas with intermingled preexisting tissue was present.

2.5.3. Histopathological parameters of anaplasia

Furthermore, detailed analysis of relevant histopathological parameters of anaplasia was conducted. To this end, histopathological variables were semiquantitatively classified into the following categories as previously described [38,40]: *Mitotic activity* (low, few or many), *nuclear pleomorphism* (low, moderate or high), *cell density* (low, moderate or high), *microvascular proliferation* (present or absent) and *focal necrosis* (present or absent).

2.6. Proliferation and MVD

Immunostaining of Ki-67 (anti-Ki-67, 1:50; DAKO) and CD34 (antibody QBEnd/10, Novacastra, Leica Biosystems, Newcastle) of 4 µm thickness tissue sections was used for analysis of tumor proliferation and MVD: (1) the monoclonal antibody MIB-1 was applied to evaluate cell proliferation and the MIB-1 proliferation index was calculated as ratio between all Ki-67 positive and negative nuclei in a maximally stained area (hotspot), including 500 cells per field (20x) and was expressed as percentage. (2) The antigen CD34 was stained for assessment of MVD with the aid of a gridded lens (20x) by the simple count of individual vessels (lumen and branches) in a hotspot and the MVD was expressed as vessels per field.

2.7. Statistical analysis

We utilized SPSS version 21 (IBM, USA) for statistical analyses. Descriptive data is presented as median and interquartile range. The FI was compared between groups using the Kruskal-Wallis test and for its correlation with continuous variables we applied the Kendall's tau correlation coefficient. To evaluate whether the FI is a discriminative marker for histopathological parameters, we calculated the area under the receiver operating characteristic (ROC) curve and defined possible cutoff points with their corresponding specificity, sensitivity, positive predictive value (PPV) and negative predictive value (NPV). Predictive cutoff values were calculated only in variables with an area under the curve (AUC) greater than 0.8. In variables with more than 2 categories cutoff values with the highest AUC were determined. Furthermore, a multivariable linear mixed model for FI values and specific histopathological parameters was fitted considering the patient as random factor and excluding non-significant variables in a backwards fashion. Because of the skewed distribution of FI, we used its logarithm as dependent variable and transformed the resulting regression coefficients back to the original scale so that the final values can be interpreted as fold changes in FI and associated 95% confidence limits. A P value below 0.05 was considered significant.

3. Results

In the present study, 76 patients with resection of a suspected diffusely infiltrating glioma (WHO grades II-IV) with assistance of 5-ALA fluorescence and additional quantitative *ex-vivo* PpIX analysis were initially included. After surgery, 8 patients had to be excluded from final analysis due to a histopathological diagnosis other than a diffusely infiltrating glioma (three lymphomas, two pilocytic astrocytomas, one ganglioglioma, one tumefactive multiple sclerosis plaque and one inflammatory lesion induced by echinococcosis). Thus, 68 patients (43 WHO grade IV, 14 WHO grade III and 11 WHO grade II gliomas) constituted our final study cohort. For details concerning the patient characteristics of our final study cohort refer to Table 1 and the excluded pathologies see Table 2.

Table 1
Patient characteristic.

	n (%)
Total of patients	68 (100)
Female:male ratio	1 : 1
Median age (range)	53 (24-80)
Contrast enhancement on MRI	
None	13 (19)
Patchy / faint	7 (10)
Focal	2 (3)
Nodular	3 (4)
Ring-like	43 (63)
Histopathology	
WHO II	11 (16)
Astrocytoma	*4* (6)
Oligodenroglioma	*4* (6)
Mixed oligoastrocytoma	*3* (4)
WHO III	14 (21)
Astrocytoma	*8* (12)
Oligodenroglioma	*2* (3)
Mixed oligoastrocytoma	*4* (6)
WHO IV	43 (63)
Glioblastoma	*43*(63)

MRI…magnetic resonance imaging, WHO… World Health Organization.

Table 2
Excluded diagnosis.

Case	Histopathological diagnosis	Maximal visual fluorescence	Maximal FI value (a. u.)
1	Lesion by echinococcosis	none	0.65
2	Lymphoma	none	0.10
3	Pilocytic astrocytoma	none	1.23
4	Pilocytic astrocytoma	vague	1.38
5	Ganglioglioma	vague	3.13
6	Lymphoma	vague	3.17
7	Lymphoma	strong	10.08
8	Multiple sclerosis plaque	strong	11.88

3.1. Tissue samples

During resection with assistance of 5-ALA fluorescence, 181 fluorescing and non-fluorescing tissue samples were collected in the 68 glioma patients. To enable analysis of visible and quantitative fluorescence in tumor tissue of diffusely infiltrating gliomas, samples with presence of mainly necrotic (n = 12) or hemorrhagic tissue (n = 2) as well as those lacking distinct tumor tissue (n = 24) were excluded from our study. We did not observe visible fluorescence in any of the 12 necrotic samples. However, we found increased FI values (mean FI: 0.65 a.u.; range: 0.12–1.38 a.u.) in these necrotic samples based on the measurements of our handheld probe. Altogether, 143 tumor samples from 68 patients were applied for further histopathological analysis.

3.2. Visible fluorescence and fluorescence intensity

Of all 143 tumor specimens, 61 samples showed strong fluorescence (54 samples from a WHO grade IV, 6 samples from a WHO grade III and one sample from a WHO grade II glioma). Further, 21 samples demonstrated vague fluorescence (15 samples from a WHO grade IV and 6 samples from a WHO grade III glioma). In contrast, the remaining 61 samples showed no visible fluorescence (44 samples from a WHO grade II, 5 samples from a WHO grade III and 12 samples from a WHO grade IV glioma). These 12 non-fluorescing samples were collected from 10 WHO grade IV gliomas showing all strong fluorescence as maximal fluorescence level in specific intratumoral areas during surgery. Each of these 12 specimens was collected after previous removal of all visible fluorescence in the 10 WHO grade IV gliomas and thus none of these 12 specimens did demonstrate visible fluorescence. However, our handheld spectroscopic probe was capable to detect increased levels of PpIX in all 12 specimens (median: 0.37 a.u.; range: 0.12–1.28 a.u.) despite the lack of visible fluorescence. The majority of specimens with vague fluorescence (n = 19; 91%) were collected from gliomas with significant contrast-enhancement on MRI, whereas two samples with vague fluorescence (9%) were derived from gliomas with non-significant contrast-enhancement. In contrast, most samples (n = 42; 69%) with no fluorescence were collected from gliomas with non-significant contrast-enhancement, whereas 19 non-fluorescing specimens (31%) were taken from gliomas with significant contrast-enhancement.

According to *ex-vivo* quantitative PpIX analysis by the handheld spectroscopic probe, the median FI was 19.97 a.u. (range: 15.88–26.36 a.u.) in samples with strong fluorescence, 9.42 a.u. (range: 6.03–12.62 a.u.) in samples with vague fluorescence and 0.18 a.u. (range: 0.11 – 0.33 a.u.) in samples with no fluorescence. The difference in the median FI between all three levels of visible fluorescence was found statistically significant ($p < 0.001$, see Fig. 2A).

3.3. Histopathology and fluorescence intensity

Further, specific histopathological parameters were analyzed in each tissue sample: (1) *WHO grade*: we found a significantly higher median FI in samples of WHO grade IV (FI: 16.12 a.u.; range: 6.89–23.09 a.u.) and WHO grade III (FI: 14.4 a.u.; range: 0.19–19.54 a.u.) as compared to WHO grade II (FI: 0.18 a.u.; range: 0.09 – 0.33 a.u.; $p < 0.001$; see Fig. 2B). However, we did not detect a significant difference in median FI values between samples of WHO grade III and WHO grade IV. (2) *Quality of tissue*: The median FI value was significantly higher in samples with compact tumor tissue (FI: 16.87 a.u.; range: 12.35–25.98 a.u.) as compared to diffusely infiltrated tumor tissue (FI: 0.46 a.u.; range: 0.35–9.27 a.u.; $p < 0.001$ and $p = 0.003$ in univariate and multivariate analysis, respectively). (3) *Histopathological criteria of anaplasia*: We found a significant difference in FI values in each of the analyzed histopathological parameters of anaplasia in the univariate analysis. On multivariable analysis, this difference remained significant with regard to mitotic rate, cell density, nuclear pleomorphism and microvascular proliferation. For further details see Table 3.

Finally, we determined FI cutoff values that are suitable to distinguish between the different histopathological parameters. FI cutoff values with very good diagnostic performance (AUC > 0.8) were found for mitotic rate, nuclear pleomorphism, microvascular proliferation and quality of tissue. Details on sensitivity, specificity, PPV and NPV of these FI cutoff values are provided in Table 3.

3.4. Proliferation index/MVD and fluorescence intensity

Finally, we also found a significant correlation between the proliferation rate assessed by MIB-1 labeling index and the FI values (Correlation coefficient: 0.461; $p < 0.001$; see Fig. 2C). In the multivariable analysis the MIB-1 labeling index remained significant ($p = 0.049$). In contrast, no correlation was found between MVD and the FI values (Correlation coefficient: 0.038; $p = 0.499$ see Fig. 2D). An illustrative WHO grade IV glioma with *ex-vivo* quantitative fluorescence analysis of samples with different visible fluorescence levels and corresponding histopathology, proliferation and microvessel density is shown in Fig. 3.

4. Discussion

Intraoperative visualization of 5-ALA induced PpIX fluorescence depends on identification of fluorescing brain tumor tissue with the “naked eye” using violet-blue excitation light microscopy. However, the present 5-ALA fluorescence detection method is limited by its observer

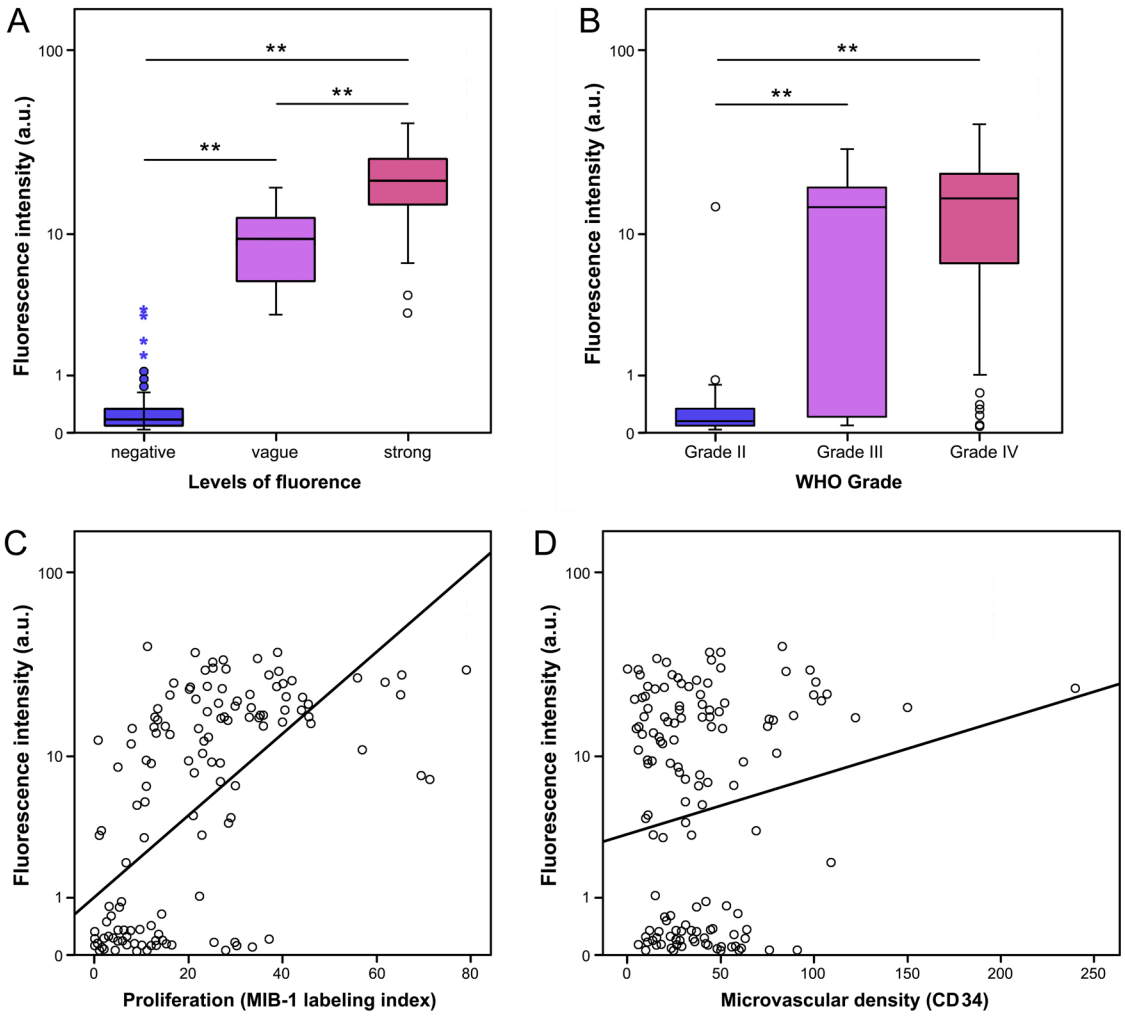

Fig. 2. Comparison of quantitative fluorescence with visible fluorescence, WHO grade, proliferation and microvacsular density.
(A) *Quantitative fluorescence and visible fluorescence*: A statistically significant difference was observed in the median fluorescence intensity (FI) between all three levels of visible fluorescence ($p < 0.001$). (B) *Quantitative fluorescence and WHO grade:* A significantly higher median FI was found in tumor samples of WHO grade III and IV as compared to WHO grade II ($p < 0.001$). However, we did not detect a significant difference in median FI values between samples of WHO grade III and IV ($p = 0.325$). (C) *Quantitative fluorescence and proliferation:* A significant linear correlation was found between FI and proliferation rate (Correlation coefficient: 0.461; $p < 0.001$). (D) *Quantitative fluorescence and microvascular density:* No significant correlation was observed between FI and microvascular density (Correlation coefficient: 0.038; $p = 0.499$).

dependence. In this sense, the semiquantitative classification in the three visible fluorescence levels (strong, vague or none) and the perception of low amounts of fluorescence might differ between various neurosurgeons [18,24,41,42]. Thus, handheld spectroscopic devices that objectively measure the 5-ALA induced PpIX accumulation in glioma tissue have been increasingly applied in the neurosurgical field in the last years [17,31,32]. Such handheld spectroscopic probes depend on the specific light properties of tissue, are easy to apply and provide reliable quantitative FI values similar to those obtained with sophisticated laboratory spectrometers [32]. So far, heterogeneous tumor entities, recurrent tumors or biopsy procedures were analyzed together in the majority of studies in the present literature using such spectroscopic devices [33,37]. Further, no detailed correlations of quantitative PpIX fluorescence with histopathology, proliferation and MVD are available in a large series of newly diagnosed diffusely infiltrating WHO grade II-IV gliomas. These data would be of major importance in order to improve tissue sampling in the future and thus result in an optimized postoperative patient management.

4.1. Present study

In the current *ex-vivo* study, we report on our initial experience with a handheld spectroscopic probe to quantitatively assess the 5-ALA induced PpIX fluorescence in large series of 68 patients with newly diagnosed diffusely infiltrating gliomas of different WHO grades.

4.1.1. Visible and quantitative fluorescence

First of all, we observed in our study significant differences in the median FI values in all three levels of visible fluorescence in newly diagnosed WHO grade II-IV gliomas. Accordingly, Stummer et al reported significant differences between visible and spectrometric fluorescence in 33 newly diagnosed WHO grade III and IV gliomas using a spectroscopic probe [33]. Similarly, Richter et al found a distinct relationship between the median fluorescence ratio measured by a handheld probe and the visible fluorescence levels classified as “none”, “weak” and “strong” fluorescence in 16 high-grade glioma patients [36]. Furthermore, Valdes et al recently described significantly higher

Table 3
Histopathological parameters and fluorescence intensity.

Histopathological parameter	*n*	Fluorescence intensity a.u. (median [IQR])	Univariate p-value	Multivariable p-value	CI 95%	Group distinction	AUC	a.u. cutoff	sens (%)	spec (%)	PPV (%)	NPV (%)
WHO Grade												
Grade II	45	0.18 (0.09 – 0.33)	p < 0.001 *	NA		WHO II vs. III / IV	0.92	1.5	88	98	99	79
Grade III	17	14.4 (0.19 – 19.54)	p = 0.325 **									
Grade IV	81	16.12 (6.89 – 23.09)	p < 0.001 ***									
Quality of tisse												
Diffusely infiltrated tumor tissue	89	0.46 (0.35 – 9.27)	< 0.001	0.003	(1.00 – 1.04)		0.818	3.18	93	63	60	93
Compact tumor tissue	54	16.87 (12.35 – 25.98)										
Histopatholigcal criteria of anaplasia												
Mitosis												
Low	12	0.18 (0.08 – 3.03)	< 0.001	0.037	(1.04 – 3.24)	Low vs. few / many	0.868	3.7	90	63	80	79
Few	72	0.42 (0.15 – 9.01)										
Many	59	18.81 (14.40-25.75)										
Cell density												
Low	28	0.28 (0.12 – 4.81)	< 0.001	0.023	(0.41 – 0.94)		< 0.8^{+}					
Moderate	64	4.31 (0.28 – 18.18)										
High	51	16.12 (7.05 – 24.68)										
Nuclear pleomorphism												
Low	41	0.24 (0.12 – 0.78)	< 0.001	0.007	(1.23 – 3.74)		0.907	2.57	98	62	57	98
Moderate	53	3.24 (0.16 – 14.54)				High vs. low/moderate						
High	49	19.71 (15.87 – 27.08)										
Microvascular Proliferation												
Abscent	83	0.32 (0.12 – 6.69)	< 0.001	0.002	(1.48 – 5.49)		0.887	1.53	98	69	69	98
Present	60	17.48 (10.50 – 24.66)										
Focal pseudopalisading necrosis												
Abscent	102	0.61 (0.16 – 14.39)	< 0.001	0.703	–		< 0.8^{+}					
Present	41	17.04 (11.31 – 24.28)										

*WHO grade II vs. III, ** WHO grade III vs. IV, *** WHO grade II vs. IV; $^{+}$AUC > 0.8 was considered as valuable for further estimation of cutoff values *a.u.*… arbitrary units, AUC… Area under the curve, *IQR*… Interquartile range, NPV… Negative predictive value, PPV… Positive predictive value, sens… sensitivity, spec… specificity, WHO…World Health Organization.

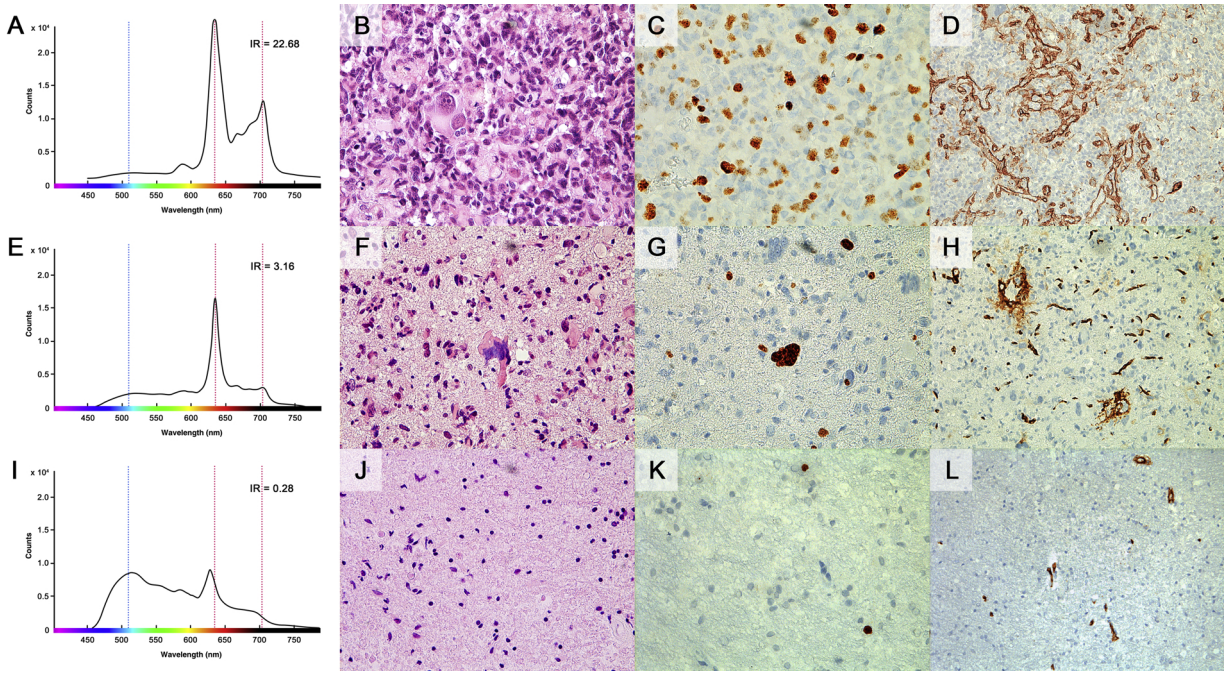

Fig. 3. Comparison of quantitative fluorescence and corresponding histopathology, proliferation and microvascular density in three samples with different visible fluorescence levels in a WHO grade IV glioma.
Sample with strong fluorescence: (A) The fluorescence intensity (FI) of a sample with strong fluorescence is very high (FI: 22.68). (B) The corresponding histopathology reveals compact tumor tissue (C) with a high proliferation rate and (D) microvessel density. *Sample with vague fluorescence*: (E) The FI of a sample with vague fluorescence is markedly increased (FI: 3.16). (F) The corresponding histopathology demonstrates infiltrated tumor tissue (G) with a medium proliferation rate and (H) microvessel density. *Sample with no fluorescence*: (I) The FI of a non-fluorescing sample is low (FI: 0.28). (J) The corresponding histopathology shows only very slight tumor infiltration with (K) a very low proliferation rate and (L) microvessel density.

PpIX concentrations in fluorescing tissue samples as compared to non-fluorescing samples in a cohort comprising 6 WHO grade I and II gliomas by application of a fiberoptic probe [37]. Moreover, Eljamel et al analyzed the FI of different visible florescence levels in gliomas and metastases with assistance of a pulsed 405 nm laser and spectrometer applying a touch probe [35]. In this study, the authors found markedly higher fluorescence ratios in areas of "red" fluorescence as compared to regions with "pink" fluorescence [35]. In sum, the reports in the literature and our data indicate that such handheld spectroscopic probes are capable to quantitatively detect distinct differences in FI values in different visible fluorescence levels. Recently, Petterssen et al described also another promising approach to distinguish different visible fluorescence levels [28]. In this study, the authors found a high intra- and interobserver reliability to differentiate between "red", "pink" and "blue" fluorescence in participants with normal colour vision by application of a "8-panel fluorescence scale" [28].

4.1.2. Quantitative FI and histopathological parameters

WHO grade: In our study, we observed significant differences in the median FI values of samples from WHO grade III/IV as compared to WHO grade II gliomas. To the best of our knowledge, this is the first study demonstrating such a difference by using a handheld spectroscopic probe in a large series of samples from newly diagnosed diffusely infiltrating WHO grade II-IV gliomas. However, we did not detect significant differences in the median FI values between samples of WHO grade III and IV gliomas. Therefore, this finding of our study represents a distinct limitation of our investigated handheld probe. One possible explanation for this might be that a similar expression of relevant enzymes/factors of the heme biosynthesis pathway responsible for intratumoral PpIX accumulation is present in WHO grade III and IV gliomas. Consequently, the expression of specific enzymes/factors of the heme biosynthesis pathway such as the ferrochelatase or coproporphyrinogen III oxidase should be further analyzed in a large series of WHO grade III and IV glioma tissue samples in future studies. It is of note, that we found, however, a high diagnostic performance of our spectroscopic probe to differentiate between samples of WHO grade II as compared to WHO grade III/IV gliomas (cutoff value: 1.5 a.u.) in our current study.

Quality of tissue: Moreover, we found significantly higher median FI values in samples with compact tumor tissue as compared to infiltrated tumor tissue. In a cohort of WHO grade III and IV gliomas, Stummer et al similarly described that strong fluorescence mostly corresponds to greater spectrometric fluorescence and "solidly proliferating tumor", whereas vague fluorescence correlated predominately to lower spectrometric fluorescence and "infiltrating tumor" [33].

Histopathological parameters of anaplasia: Furthermore, we also found significant differences in median FI values in each of the analyzed histopathological parameters of anaplasia in the univariate analysis, which remained significant with regard to mitotic rate, cell density, nuclear pleomorphism and microvascular proliferation in the multivariable analysis. In the current literature, FI values derived from spectroscopic devices were most commonly correlated to cell density. In this sense, Stummer et al found a significant correlation between tissue samples with increased cell density and high spectrometric fluorescence as well as between specimens with decreased cell density and low FI values [33]. To the best of our knowledge, a significant correlation of quantitative FI values measured by a handheld spectroscopic probe with regard to mitotic rate, nuclear pleomorphism and microvascular proliferation in a large series of newly diagnosed diffusely infiltrating WHO grade II-IV gliomas was not described so far.

4.1.3. Quantitative FI and proliferation

In our study, we observed a significant correlation between the proliferation rate assessed by MIB-1 labeling index and the FI values. Accordingly, Ishihara et al described a strong correlation between the FI ratio and proliferation in 6 WHO grade II-IV gliomas by application of visual light spectroscopy [43]. In this study, proliferation was the only significant variable remaining after multivariable analysis further including CD31-MVD and vascular endothelial growth factor (VEGF) [43].

4.1.4. Quantitative FI and microvascular density

Finally, we did not find a significant correlation between MVD and the FI values in our study. In contrast, Ishihara et al detected in their study a significant correlation between the FI ratio and the CD31-MVD in the 6 WHO grade II-IV gliomas [43]. However, this difference did not remain significant in the multivariable analysis [43].

4.2. Relevance and future perspectives

5-ALA fluorescence-guided surgery represents a powerful, safe and cost-effective technique to improve neurosurgical procedures [27]. According to our data, handheld spectroscopic probes are capable to detect distinct differences in FI values between visible fluorescence levels and are thus a further improvement of the current 5-ALA technique to objectify assessment of 5-ALA induced PpIX accumulation in WHO grade II-IV gliomas. Furthermore, such probes are also able to visualize intratumoral histopathological heterogeneity especially with regard to specific histopathological parameters and proliferation in gliomas. Thus, the future intraoperative use of this handheld spectroscopic probe will standardize the assessment of fluorescence during glioma resection. Moreover, we expect to markedly improve the precision of tissue sampling during glioma surgery by application of our determined cutoff values in order to visualize areas of focal malignant transformation that might remain undetected by visible fluorescence alone.

4.3. Limitations

Our study is associated with specific limitations. (1) First of all, the diffusely infiltrating gliomas included in our study were not classified according to the updated histopathological WHO 2016 criteria. However, all patients were included before the release of the updated WHO 2016 criteria and thus all tumors were classified according to the applicable histopathological WHO criteria at time of diagnosis [39]. (2) Furthermore, we did not measure the FI values of "normal tissue" serving as a negative control and did not analyze the diagnostic performance of our spectroscopic probe (PpIX analysis for definition of the tumor margin) since we did not perform sampling of "normal" brain tissue only for the *ex-vivo* analysis of FI values due to ethical concerns. Moreover, the scope of this study was to correlate the FI values with histopathology, proliferation and MVD in tumor tissue of diffusely infiltrating gliomas of various WHO grades. (3) Finally, we did not systematically correlate the location of each collected sample with the specific region (e.g. infiltrative margin vs tumor bulk) in each tumor assessed by neuronavigation. However, this was not the scope of the present study. Future studies should topographically correlate the site of tissue collection of samples with different visual fluorescence/FI values with specific tumor locations assessed by neuronavigation.

5. Conclusions

In the present *ex-vivo* study, we report on our initial experience with a handheld spectroscopic probe to quantitatively assess the 5-ALA induced PpIX fluorescence in large cohort of newly diagnosed WHO grade II-IV gliomas. According to our data, quantitative fluorescence correlates with visible fluorescence, histopathological parameters and proliferation. Therefore, such handheld probes allow visualizing intratumoral glioma heterogeneity by objective assessment of fluorescence. The future intraoperative application of such devices will thus markedly support the neurosurgeon to improve tissue sampling in newly diagnosed gliomas in order to optimize postoperative patient management.

Disclosure of interest

Stefan Wolfsberger is currently educational consultant and technological advisory board member of Medtronic. The other authors have no personal financial or institutional interest in any of the drugs, materials, or devices described in this article.

Acknowledgements

For the current study M. Martínez-Moreno was granted by the National Council of Sciences and Technology of Mexico (Conacyt; Register 218137). This study was performed within the PhD thesis project of Clinical Neuroscience (CLINS) at the Medical University Vienna. We thank Prof. Georg Heinze for statistical advice, Ola Svärm for technical assistance regarding the spectroscopic probe and Ingrid Dobsak for graphical support.

References

[1] L.M. DeAngelis, L.M. DeAngelis, Brain Tumors, N. Engl. J. Med. 344 (2001) 114–123.
[2] T.A. Dolecek, J.M. Propp, N.E. Stroup, C. Kruchko, CBTRUS statistical report: primary brain and central nervous system tumors diagnosed in the United States in 2005-2009, Neuro-Oncology. 14 (2012) v1–v49.
[3] D.N. Louis, A. Perry, G. Reifenberger, A. von Deimling, A. Deimling, D. Figarella-Branger, et al., The 2016 World Health Organization classification of tumors of the central nervous system: a summary, Acta Neuropathol. 131 (2016) 803–820.
[4] D.J. Aum, D.H. Kim, T.L. Beaumont, E.C. Leuthardt, G.P. Dunn, A.H. Kim, Molecular and cellular heterogeneity: the hallmark of glioblastoma, Neurosurg. Focus 37 (2014) E11–11.
[5] P. Birner, M. Piribauer, I. Fischer, B. Gatterbauer, C. Marosi, P.F. Ambros, et al., Vascular patterns in glioblastoma influence clinical outcome and associate with variable expression of angiogenic proteins: evidence for distinct angiogenic subtypes, Brain Pathol. 13 (2003) 133–143.
[6] T.J. Brown, M.C. Brennan, M. Li, E.W. Church, N.J. Brandmeir, K.L. Rakszawski, et al., Association of the extent of resection with survival in glioblastoma, JAMA Oncol. 2 (2016) 1460–1510.
[7] M.L. Goodenberger, R.B. Jenkins, Genetics of adult glioma, Cancer Genet. 205 (2012) 613–621.
[8] W. Paulus, J. Peiffer, Intratumoral histologic heterogeneity of gliomas, A quantitative study 64 (1989) 442–447.
[9] S. Popov, A. Jury, R. Laxton, L. Doey, N. Kandasamy, S. Al-Sarraj, et al., IDH1-associated primary glioblastoma in young adults displays differential patterns of tumour and vascular morphology, PLoS One 8 (2013) e56328–7.
[10] M.S. N. Sanai, Berger, glioma extent of resection and its impact on patient outcome, Neurosurgery 62 (2008) 753–766.
[11] C. Watts, S.J. Price, T. Santarius, Current concepts in the surgical management of glioma patients, Clin. Oncol. 26 (2014) 385–394.
[12] H. Duffau, E. Mandonnet, The “onco-functional balance” in surgery for diffuse low-grade glioma: integrating the extent of resection with quality of life, Acta Neurochir. (Wien) 155 (2013) 951–957.
[13] N.F. Marko, N.F. Marko, R.J. Weil, R.J. Weil, J.L. Schroeder, J.L. Schroeder, et al., Extent of resection of glioblastoma revisited: personalized survival modeling facilitates more accurate survival prediction and supports a maximum-safe-Resection approach to surgery, Jco. 32 (2014) 774–782.
[14] C. Ewelt, F.W. Floeth, J. Felsberg, H.J. Steiger, M. Sabel, K.-J. Langen, et al., Finding the anaplastic focus in diffuse gliomas: the value of Gd-DTPA enhanced MRI, FET-PET, and intraoperative, ALA-derived tissue fluorescence, Clin. Neurol. Neurosurg. 113 (2011) 541–547.
[15] G. Widhalm, S. Wolfsberger, G. Minchev, A. Woehrer, M. Krssak, T. Czech, et al., 5-Aminolevulinic acid is a promising marker for detection of anaplastic foci in diffusely infiltrating gliomas with nonsignificant contrast enhancement, Cancer 116 (2010) 1545–1552.
[16] C.G. Hadjipanayis, G. Widhalm, W. Stummer, What is the surgical benefit of utilizing 5-aminolevulinic acid for fluorescence-guided surgery of malignant gliomas? Neurosurgery 77 (2015) 663–673.
[17] P.A. Valdes, F. Leblond, A. Kim, B.T. Harris, B.C. Wilson, X. Fan, et al., Quantitative fluorescence in intracranial tumor: implications for ALA-induced PpIX as an intraoperative biomarker, J. Neurosurg. 16 (2011) 11–17.
[18] P.A. Valdes, D.W. Roberts, F.-K. Lu, A. Golby, Optical technologies for intraoperative neurosurgical guidance, Neurosurg. Focus 8 (2016) E8-35.
[19] R.D. Valle, Established and emerging uses of 5-ALA in the brain: an overview, J. Neurooncol. (2019).
[20] W. Stummer, U. Pichlmeier, T. Meinel, O.D. Wiestler, F. Zanella, H.J. Reulen, Fluorescence-guided surgery with 5-aminolevulinic acid for resection of malignant glioma: a randomised controlled multicentre phase III trial, Lancet Oncol. 7 (2006) 392–401.
[21] Q. Peng, T. Warloe, K. Berg, J. Moan, M. Kongshaug, K.E. Giercksky, et al., 5-Aminolevulinic acid-based photodynamic therapy. Clinical research and future challenges, Cancer 79 (1997) 2282–2308.
[22] Q. Peng, K. Berg, J. Moan, M. Kongshaug, J.M. Nesland, 5-Aminolevulinic acid-based photodynamic therapy: principles and experimental research, Photochem. Photobiol. 65 (1997) 235–251.
[23] W. Stummer, H. Stepp, G. Möller, A. Ehrhardt, M. Leonhard, H.J. Reulen, Technical principles for Protoporphyrin-IX-Fluorescence guided microsurgical resection of malignant glioma tissue, Acta Neurochir. (Wien) 140 (1998) 995–1000.
[24] M.A. Kamp, Z. Krause Molle, Z.K. Molle, C. Munoz-Bendix, M. Rapp, M. Sabel, et al., Various shades of red—a systematic analysis of qualitative estimation of ALA-derived fluorescence in neurosurgery, Neurosurg. Rev. 41 (2016) 3–18.
[25] D. Lau, S.L. Hervey-Jumper, S. Chang, A.M. Molinaro, M.W. McDermott, J.J. Phillips, et al., A prospective Phase II clinical trial of 5-aminolevulinic acid to assess the correlation of intraoperative fluorescence intensity and degree of histologic cellularity during resection of high-grade gliomas, J. Neurosurg. 2014 (2016) 1300–1309.
[26] G. Widhalm, Intraoperative visualization of brain tumors with 5-aminolevulinic acid-induced fluorescence, Clin. Neuropathol. 33 (2014) 260–278.
[27] S. Kaneko, M.S. Eljamel, Fluorescence image-guided neurosurgery, Future Oncology 13 (2017) 2341–2348.
[28] M. Petterssen, S. Eljamel, MD, Sam Eljamel MBBCh, Protoporphyrin-IX fluorescence guided surgical resection in high-grade gliomas: The potential impact of human colour perception, Photodiagnosis and Photodynamic Therapy (2014) 1–6.
[29] B. Kiesel, M. Mischkulnig, A. Woehrer, M. Martínez-Moreno, M. Millesi, A. Mallouhi, et al., Systematic histopathological analysis of different 5-aminolevulinic acid–induced fluorescence levels in newly diagnosed glioblastomas, J. Neurosurg. 17 (2017) 341–353.
[30] J.C.O. Richter, N. Haj-Hosseini, S. Andersson-Engel, K. Wårdell, Fluorescence spectroscopy measurements in ultrasonic navigated resection of malignant brain tumors, Lasers Surg. Med. 43 (2011) 8–14.
[31] N. Haj-Hosseini, J. Richter, S. Andersson-Engels, K. Wårdell, Optical touch pointer for fluorescence guided glioblastoma resection using 5-aminolevulinic acid, Lasers Surg. Med. 42 (2010) 9–14.
[32] J.F. Cornelius, J.M. Placke, J. Knipps, I. Fischer, M. Kamp, H.J. Steiger, Minispectrometer with handheld probe for 5-ALA based fluorescence-guided surgery of brain tumors: preliminary study for clinical applications, Photodiagnosis Photodyn. Ther. 17 (2017) 147–153.
[33] W. Stummer, J.-C. Tonn, C. Goetz, W. Ullrich, H. Stepp, A. Bink, et al., 5-aminolevulinic acid-derived tumor fluorescence: the diagnostic accuracy of visible fluorescence qualities as corroborated by spectrometry and histology and post-operative imaging, Neurosurgery. 74 (2014) 310–320.
[34] P.A. Valdes, F. Leblond, V.L. Jacobs, B.C. Wilson, K.D. Paulsen, D.W. Roberts, Quantitative, spectrally-resolved intraoperative fluorescence imaging, Sci. Rep. 2 (2012) 603.
[35] S. Eljamel, M. Petersen, R. Valentine, R. Buist, C. Goodman, H. Moseley, et al., Comparison of intraoperative fluorescence and MRI image guided neuronavigation in malignant brain tumours, a prospective controlled study, Photodiagnosis and Photodynamic Therapy (2013) 1–6.
[36] J.C.O. Richter, N. Haj-Hosseini, M. Hallbeck, K. Wårdell, Combination of hand-held probe and microscopy for fluorescence guided surgery in the brain tumor marginal zone, Photodiagnosis Photodyn. Ther. 18 (2017) 185–192.
[37] P.A. Valdes, V. Jacobs, B.T. Harris, B.C. Wilson, F. Leblond, K.D. Paulsen, et al., Quantitative fluorescence using 5-aminolevulinic acid-induced protoporphyrin IX biomarker as a surgical adjunct in low-grade glioma surgery, J. Neurosurg. 30 (2015) 771–780.
[38] B. Kiesel, M. Mischkulnig, A. Woehrer, M. Martínez-Moreno, M. Millesi, A. Mallouhi, et al., Systematic histopathological analysis of different 5-aminolevulinic acid–induced fluorescence levels in newly diagnosed glioblastomas, J. Neurosurg. 17 (2019) 341–353.
[39] D.N. Louis, H. Ohgaki, O.D. Wiestler, W.K. Cavenee, P.C. Burger, A. Jouvet, et al., The 2007 WHO Classification of Tumours of the Central Nervous System, Acta Neuropathol. 114 (2007) 97–109.
[40] G. Widhalm, B. Kiesel, A. Woehrer, T. Traub-Weidinger, M. Preusser, C. Marosi, et al., 5-aminolevulinic acid induced fluorescence is a powerful intraoperative marker for precise histopathological grading of gliomas with non-significant contrast-enhancement, PLoS One 8 (2013) e76988.
[41] J.T.C. Liu, D. Meza, N. Sanai, Trends in fluorescence image-guided surgery for gliomas, Neurosurgery 75 (2014) 61–71.
[42] W. Stummer, W. Stummer, A. Novotny, A. Novotny, H. Stepp, H. Stepp, et al., Fluorescence-guided resection of glioblastoma multiforme utilizing 5-ALA-induced porphyrins: a prospective study in 52 consecutive patients, J. Neurosurg. 34 (2000) 1003–1013.
[43] R. Ishihara, Y. Katayama, T. Watanabe, A. Yoshino, T. Fukushima, K. Sakatani, Quantitative spectroscopic analysis of 5-aminolevulinic acid-induced protoporphyrin IX fluorescence intensity in diffusely infiltrating astrocytomas, Neurol. Med. Chir. 47 (2007) 53–7– discussion 57.